Available online at www.sciencedirect.com
ScienceDirect
Journal of Power Sources 166 (2007) 22–29
JOURNAL OF POWER SOURCES
www.elsevier.com/locate/jpowsour

Electrical conductivity of cobalt doped $La_{0.8}Sr_{0.2}Ga_{0.8}Mg_{0.2}O_{3-\delta}$

Shizhong Wang *, Lingli Wu, Ying Liang

Department of Chemistry, Xiamen University, Xiamen 361005, Fujian, PR China

Received 8 November 2006; received in revised form 15 December 2006; accepted 15 December 2006
Available online 17 January 2007

Abstract

$La_{0.8}Sr_{0.2}Ga_{0.8}Mg_{0.2}O_{3-\delta}$ (LSGM8282), $La_{0.8}Sr_{0.2}Ga_{0.8}Mg_{0.15}Co_{0.05}O_{3-\delta}$ (LSGMC5) and $La_{0.8}Sr_{0.2}Ga_{0.8}Mg_{0.115}Co_{0.085}O_{3-\delta}$ (LSGMC8.5) were prepared using a conventional solid-state reaction. Electrical conductivities and electronic conductivities of the samples were measured using four-probe impedance spectrometry, four-probe dc polarization and Hebb–Wagner polarization within the temperature range of 973–1173 K. The electrical conductivities in LSGMC5 and LSGMC8.5 increased with decreasing oxygen partial pressures especially in the high ($>10^{-5}$ atm) and low oxygen partial pressure regions ($<10^{-15}$ atm). However, the electrical conductivity in LSGM8282 had no dependency on the oxygen partial pressure. At temperatures higher than 1073 K, P_{O_2} dependencies of the free electron conductivities in LSGM8282, LSGMC5 and LSGMC8.5 were about −1/4, and P_{O_2} dependencies of the electron hole conductivities were about 0.25, 0.12 and 0.07, respectively. Oxygen ion conductivities in LSGMC5 and LSGMC8.5 increased with decreasing oxygen partial pressures especially in the high and low oxygen partial pressure regions, which was due to the increase in the concentration of oxygen vacancies. The change in the concentration of oxygen vacancies and the valence of cobalt with oxygen partial pressure were determined using a thermo-gravimetric technique. Both the electronic conductivity and oxygen ion conductivity in cobalt doped lanthanum gallate samples increased with increasing concentration of cobalt, suggesting that the concentration of cobalt should be optimized carefully to maintain a high electrical conductivity and close to 1 oxygen ion transference number.

Keywords: Electrical conductivity; Hebb–Wagner polarization; Oxygen ion conductivity; Oxygen vacancy; Lanthanum gallate

1. Introduction

Oxygen ion conductors with high electrical conductivity are important candidates for electrolytes in solid oxide fuel cells (SOFCs) [1–8]. Cobalt doped $La_{0.8}Sr_{0.2}Ga_{0.8}Mg_{0.2}O_{3-\delta}$ (LSGM8282) perovskites show superior oxygen ion conductivity and good chemical stability [3,6–8], and are regarded as promising candidates for the electrolyte of intermediate temperature solid oxide fuel cells (ITSOFCs).

Efficiency of SOFCs is closely related to the electronic conductivity of the electrolyte, since the minor charge carriers in the electrolyte, i.e., free electrons and electron holes, could lead to a short circuit current [2,9]. The studies of the conductivity of LSGM8282 with a low concentration of cobalt (<8.5 mol%) are still very limited [6–8]. Ishihara et al. [7] investigated the electronic conductivity in cobalt doped LSGM8282 with the ion blocking method. Electronic conductivities at various temperatures in $La_{0.8}Sr_{0.2}Ga_{0.8}Mg_{0.15}Co_{0.05}O_{3-\delta}$ (LSGMC5) and electronic conductivities at 1073 K in LSGM8282 doped with various amount of cobalt were reported. It was considered that the extrinsic free electron and electron hole conductivity caused by the redox reactions involving doped cobalt became dominant with decreasing temperatures [8].

Despite the limitations in the number of studies of the conductivity of lanthanum gallate, there are obvious discrepancies among the results reported [6–8,10]. The accuracy of the Hebb–Wagner polarization measurement depends strongly on the operational conditions. It is essential to maintain good sealing of the blocking electrode compartment. Further, special care should be taken to prevent the diffusion of oxygen from the reversible electrode compartment to the blocking electrode compartment [7]. It would be helpful to verify the operating systems by checking some well-studied samples.

The properties of the electrolyte have a strong effect on the polarization resistance of the electrode supported on the electrolyte beside the dominant effect on the ohmic resistance of the cell [11,12]. The cells based on cobalt doped lanthanum gallate exhibited a superior low ohmic resistance and electrode

* Corresponding author. Tel.: +86 592 2184968; fax: +86 592 2184948.
E-mail address: shizwang@sohu.com (S. Wang).

0378-7753/$ – see front matter © 2007 Elsevier B.V. All rights reserved.
doi:10.1016/j.jpowsour.2006.12.090

polarization resistance compared with the cells supported on $La_{0.9}Sr_{0.1}Ga_{0.8}Mg_{0.2}O_{3-\delta}$. $La_{0.8}Sr_{0.2}Ga_{0.8}Mg_{0.115}Co_{0.085}O_{3-\delta}$ exhibited the highest performance among the cobalt doped LSGM8282 electrolytes [12]. It was assumed that the properties of the charge carriers in the electrolyte could play a major role in determining the cell performance. The study of the defects in cobalt doped lanthanum gallate is an important topic, which is closely related to the conductivity of the materials. The decrease in the valence of Co and the increase in the concentration of oxygen vacancies with decreasing oxygen partial pressures of Co doped lanthanum gallate have been characterized using redox titration [8], and a significant oxygen partial pressure dependency of the concentration of oxygen vacancies was observed. However, no effect of oxygen partial pressure on the oxygen ion conductivity in cobalt doped LSGM8282 was reported. This is quite questionable considering that the oxygen ion conductivity should be closely related to the concentration of oxygen vacancies. It would be interesting to further study the electrical conductivity and defect equilibrium in cobalt doped lanthanum gallate in detail.

In this study, three typical lanthanum gallate electrolytes, i.e., LSGM8282, LSGMC5 and LSGMC8.5, were prepared using the conventional solid-state reaction. Electrical conductivities and electronic conductivities of the samples were measured using four-probe impedance spectrometry, four-probe dc polarization and Hebb–Wagner polarization within the temperature range of 973–1173 K. The re-examination of LSGM8282, which is a well-studied material, was to verify the experimental conditions. The change in the concentration of oxygen vacancies and the valence of cobalt with decreasing oxygen partial pressures were determined using thermo-gravimetric technique.

2. Experimental

$La_{0.8}Sr_{0.2}Ga_{0.8}Mg_{0.2}O_{3-\delta}$ (LSGM8282), $La_{0.8}Sr_{0.2}Ga_{0.8}Mg_{0.15}Co_{0.05}O_{3-\delta}$ (LSGMC5) and $La_{0.8}Sr_{0.2}Ga_{0.8}Mg_{0.115}Co_{0.085}O_{3-\delta}$ (LSGMC8.5) were prepared using the conventional solid-state reaction. The precursors of the samples were La_2O_3 (99.99%), $SrCO_3$ (99.5%), MgO (99.5%), Ga_2O_3 (99.99%) and CoO (99.99%). Powders of the precursors in stoichiometric ratio were ball-milled for 24 h. The mixture was then pre-calcined at 1273 K for 6 h, after which the pre-calcined mixture was iso-statically pressed into a disk at 274.6 MPa for 10 min. The diameter of the green disk was 2.0 cm. The disks were then sintered at 1773 K for 6 h in air. The sintered disks were polished to a thickness of 1 mm. The phase compositions of the materials were identified using XRD (Panalytical X'pert).

The densities of the sintered disks were measured using the Archimedes technique, and the densities of LSGM8282, LSGMC5 and LSGMC8.5 were 6.39, 6.53 and 6.59 g cm^{-3}, respectively, showing relative densities higher than 98%.

The sintered disks were cut into a rectangular shape for electrical conductivity measurements. The dimension of the samples was typically 2 mm × 1 mm × 15 mm. Platinum paste was applied to both end of the bar and calcined at 1173 K for 30 min as working and counter electrode. Two platinum wires were attached to the bar close to the working and counter electrode, respectively, as two reference electrodes. The electrical conductivities were measured as a function of temperature in a mixture of N_2 (99.99%) and water saturated H_2 (99.99%), or oxygen (99.99%) and N_2 (99.99%) by using a VMP2/Z-40 electrochemical testing station (AMETECH). The oxygen partial pressure was determined using a zirconia oxygen sensor. The flow rate of the gas mixture was about 100 ml min^{-1}. The electrical conductivities were measured by using both the four-probe impedance spectrometry and four-probe dc polarization, the results of which agreed with each other well.

Electronic conductivity was measured using the Hebb–Wagner polarization method [13–15]. Ion-blocking polarization cells of the configuration.

Dense Al_2O_3 plate, Pt (blocking electrode)/sample/Pt (reversible electrode), air were constructed [7–8,10]. Pt paste was painted on both faces of the samples symmetrically with a diameter about 10 mm and sintered at 1173 K for 30 min. The blank surface of the sample was covered with powders of Pyrex glass to prevent the diffusion of oxygen from the reversible electrode compartment to the blocking electrode compartment. Pyrex glass powder as well as Pyrex glass ring was used for the sealing between the dense alumina plate and the sample, and between the sample and an alumina tube. The mixture of high purity (99.99%) N_2 and O_2 with an oxygen partial pressure about 0.21 atm was used as the reference gas passing over the reversible electrode. The feeding rate of the gas was about 100 ml min^{-1}. A constant dc voltage was applied on the sample by using a VMP2/Z-40 electrochemical testing station (AMETECH), and the residual current was measured using the same equipment.

The weight losses in nitrogen of LSGM8282, LSGMC5 and LSGMC8.5 were measured using thermo-gravimetric analyses technique (Netzsh STA409) as a function of temperature. The samples were prepared as follows. Powders of the samples were sintered at 1773 K for 6 h, and then ground into fine powders. Before the measurements, the powders were calcined in air or oxygen for 2 h at 1073 K and then quenched to room temperature quickly. Six samples were tested, which were abbreviated as LSGM8282-air, LSGM8282-oxygen, LSGMC5-air, LSGMC5-oxygen, LSGMC8.5-air and LSGMC8.5-oxygen. The weight losses of the samples were measured in 50 ml min^{-1} flowing high purity nitrogen. Oxygen partial pressure of the high purity nitrogen was about 1×10^{-5} atm as determined by the zirconium oxygen sensor. Three heating rates were tested, i.e., 10, 5 and 2 K min^{-1}. The weight loss measured using a heating rate of 5 K min^{-1} was the same as that of 2 K min^{-1}, which exhibited a relative error within 1–2% compared with that using a heating rate of 10 K min^{-1}. Therefore, the weight losses under a heating rate of 5 K min^{-1} were reported in this study.

3. Results

3.1. Phase composition

The XRD patterns of LSGM8282, LSGMC5 and LSGMC8.5 are shown in Fig. 1. The results show that the samples exhibit the same single phase resembling that of $La_{0.9}Sr_{0.1}Ga_{0.8}Mg_{0.2}O_{2.87}$.

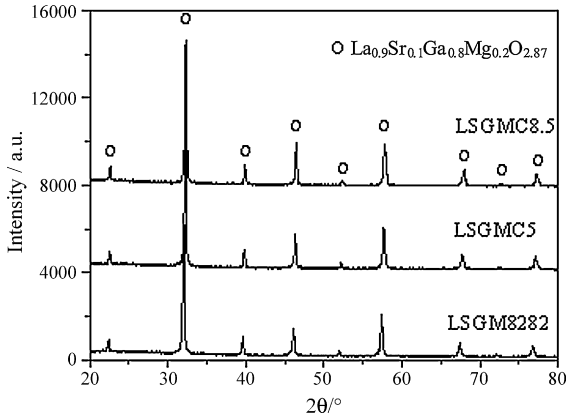

Fig. 1. XRD patterns of LSGM8282, LSGMC5 and LSGMC8.5.

No apparent impurities can be identified in Fig. 1. With the increase in the concentration of cobalt in the samples, the peaks shift towards higher 2θ. This suggests that a part of the Mg^{2+} ions are replaced by the small Co^{3+} ions [8].

3.2. Electrical conductivity

Shown in Fig. 2 are the impedance spectra of LSGM8282 and LSGMC5 cells for electrical conductivity measurements under various oxygen partial pressures at 1073 K. It can be seen from Fig. 2 that the impedances of the two cells do not change with the frequency of the ac signal within the frequency range of 1 kHz–10 Hz. Further, the real part of the impedance spectra is exactly the same as that measured using four-probe dc polarization method. Therefore, the resistances of the electrolyte are determined using the real part of the impedance at 100 Hz, from which the electrical conductivities can be estimated. Fig. 2 shows clearly that the electrical conductivity of LSGMC5 is strongly dependent on the partial pressure of oxygen especially under high and low oxygen partial pressures, while the conductivity of LSGM8282 is independent of oxygen partial pressure.

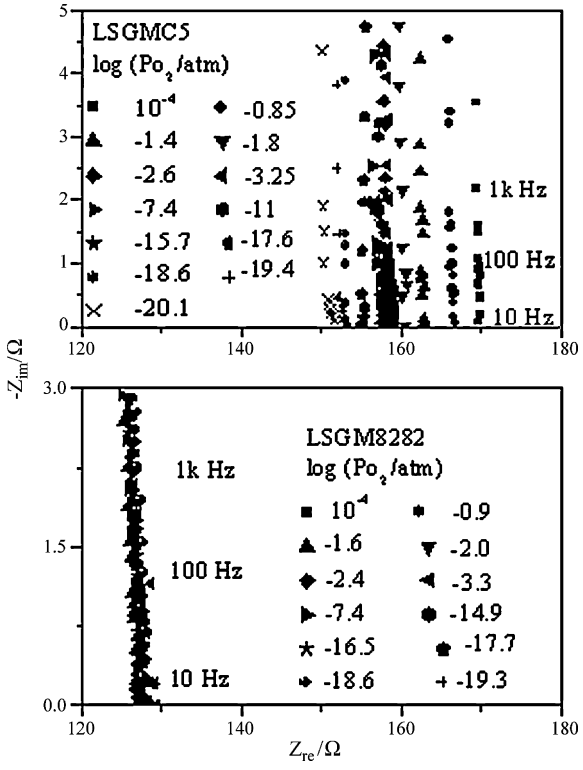

Fig. 2. Impedance spectra under various oxygen partial pressures at 1073 K of LSGM8282 and LSGMC5 cells used for electrical conductivity measurements.

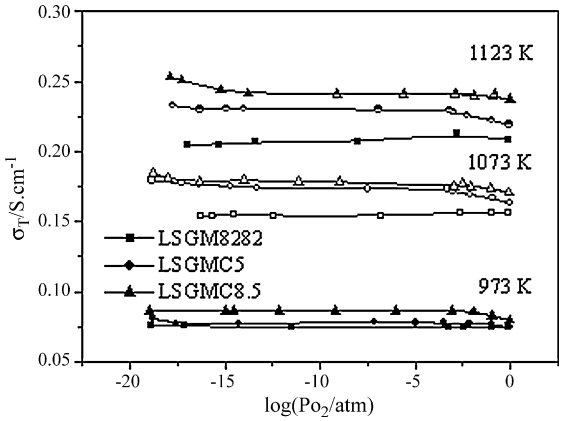

Fig. 3. Electrical conductivities in LSGM8282, LSGMC5 and LSGMC8.5 as a function of oxygen partial pressure at various temperatures.

The electrical conductivities in LSGM8282, LSGMC5 and LSGMC8.5 at 973, 1073 and 1123 K under various oxygen partial pressures are shown in Fig. 3. It is obvious that the electrical conductivities of LSGMC5 and LSGMC8.5 increase with decreasing oxygen partial pressures at various temperatures especially in low ($<10^{-15}$ atm) and high oxygen partial pressure regions ($>10^{-5}$ atm). For an example, the electrical conductivity in LSGMC5 is about 0.16 S cm^{-1} in oxygen at 1073 K, and increases to about 0.17 S cm^{-1} at 10^{-5} atm oxygen partial pressure and 0.18 S cm^{-1} at 10^{-19} atm oxygen partial pressure. To our knowledge, this is the first report on the significant P_{O_2} dependency of the electrical conductivity in LSGMC5 and LSGMC8.5. Electrical conductivity in LSGM8282 shows no dependency on oxygen partial pressure within the oxygen partial pressure range studied.

The electrical conductivities of the samples are in the order of LSGM8282 < LSGMC5 < LSGMC8.5 at various temperatures, which is the same as that reported in the literature [7]. It is clear that the substitution of magnesium with cobalt can increase the conductivity in LSGM8282 significantly. Further, the addition of cobalt has a strong effect on the oxygen partial pressure dependency of the electrical conductivity.

3.3. Electronic conductivity

Electronic conductivities in LSGM8282, LSGMC5 and LSGMC8.5 were measured using Hebb–Wagner polarization within the temperature range of 973–1173 K. As a typical example, the residual current I against the voltage U of various samples at 1073 K are shown in Fig. 4. U is defined as the potential of the reversible electrode relative to the blocking electrode. For LSGM8282, the I–U curves are typical S shape, which can be well fitted using the traditional Hebb–Wagner polarization

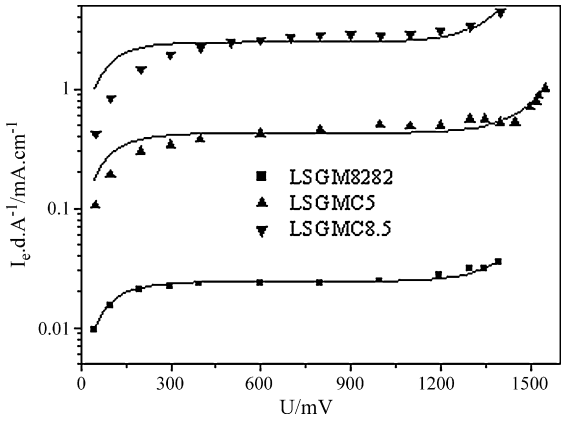

Fig. 4. *I–U* curves of the ion-blocking cell involving LSGM8282, LSGMC5 and LSGMC8.5 at 1073 K. Point-experimental and line-simulated.

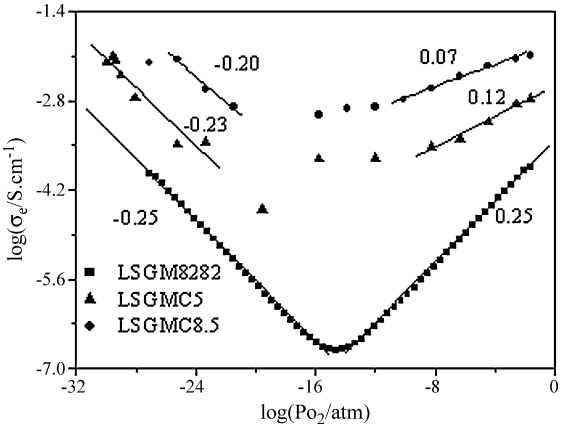

Fig. 5. Electronic conductivities in LSGM8282, LSGMC5 and LSGMC8.5 as a function of oxygen partial pressure at 1073 K.

equation (Eq. (1)) as shown in Fig. 4.

$$I_e = \frac{RT}{F}\frac{A}{d}\left(\sigma'_p\left(1-\exp\left(-\frac{UF}{RT}\right)\right) + \sigma'_n\left(\exp\left(\frac{UF}{RT}\right)-1\right)\right) \quad (1)$$

Here, I_e, R, T and F are the residual current measured, gas constant, temperature and Faraday constant, respectively. A and d denote the cross sectional area and thickness of the specimen, respectively. σ'_p and σ'_n are the p-type and n-type conductivity, respectively, at the reference oxygen activity at the reversible electrode.

Eq. (1) can be obtained easily taking into account of the charge equilibrium in LSGM8282 (Eq. (2)), the redox reaction (Eq. (3)), and the electronic excitation reaction equilibrium (Eq. (4)) [10]

$$2[V_O^{\bullet\bullet}] \approx [Sr'_{La}] + [Mg'_{Ga}] \quad (2)$$

$$O_O^X = \tfrac{1}{2}O_2 + V_O^{\bullet\bullet} + 2e' \quad (3)$$

$$0 = e' + h^{\bullet} \quad (4)$$

Electron hole conductivity (σ_p) and free electron conductivity (σ_n) of the samples can be written as [10]

$$\sigma_p = \sigma'_p\left(\frac{a_{O_2}}{a'_{O_2}}\right)^{1/4} \quad (5)$$

$$\sigma_n = \sigma'_n\left(\frac{a_{O_2}}{a'_{O_2}}\right)^{-1/4} \quad (6)$$

a_{O_2} and a'_{O_2} are oxygen activity at the blocking electrode and the reversible electrode, respectively. a_{O_2}, which is close to the oxygen partial pressure at the blocking electrode at high temperatures, can be estimated using Nernst equation (Eq. (7)) considering that the oxygen partial pressure of the reference gas is 0.21 atm [10].

$$a_{O_2} = 0.21\exp\left(-\frac{4UF}{RT}\right) \quad (7)$$

Since the *I–U* curves of LSGMC5 and LSGMC8.5 do not agree with Eq. (1) as shown in Fig. 4, the electronic conductivities are calculated using Eq. (8) [7,8].

$$\sigma_e = \frac{d}{A}\left(\frac{\partial I}{\partial U}\right) \quad (8)$$

Shown in Fig. 5 are the electronic conductivities of LSGM-8282, LSGMC5 and LSGMC8.5 extracted from Fig. 4 using Eqs. (2), (5) and (6) or Eq. (8). The electronic conductivities in the samples decrease with decreasing oxygen partial pressures in high oxygen partial pressure region while increase in low oxygen partial pressure region, which correspond to electron hole conduction and free electron conduction, respectively. P_{O_2} dependencies of the free electron conduction show no obvious dependency on the amount of cobalt in the sample, which are about −1/4. However, the P_{O_2} dependencies of electron hole conduction decrease with increasing concentration of cobalt in the sample, which are about 0.25, 0.12 and 0.07 for LSGM8282, LSGMC5 and LSGMC8.5, respectively. It can also be observed from Fig. 5 that both the free electron conductivity and electron hole conductivity in cobalt doped LSGM8282 increase with increasing concentration of cobalt as reported in the literature [7].

Shown in Fig. 6 are the electronic conductivities of LSGM-8282 at various temperatures calculated using Eqs. (2), (5) and (6). P_{O_2} dependencies of the free electron and electron hole conductivity in LSGM8282 are −1/4 and 1/4, respectively, at various temperatures. It can also be observed from Fig. 6 that the electronic conductivity in LSGM8282 increases with increasing temperatures.

Shown in Fig. 7 are the electronic conductivities in LSGMC5 at various temperatures calculated using Eq. (8). P_{O_2} dependencies of the electronic conductivities in LSGMC5 depend strongly on working temperatures. At 973 K, the P_{O_2} dependencies of free electron conductivity and electron hole conductivity are about −0.16 and 0.084, respectively. However, at temperatures higher than 1073 K, the P_{O_2} dependencies of free electron conductivity and electron hole conductivity are all about −1/4 and 1/8, respectively.

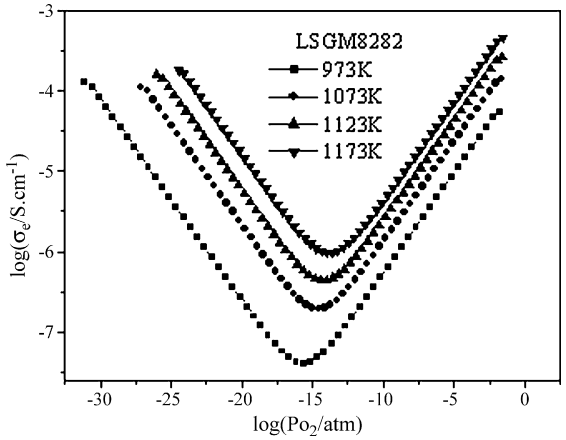

Fig. 6. Electronic conductivities in LSGM8282 as a function of oxygen partial pressure at various temperatures.

Shown in Fig. 8 are the electronic conductivities in LSGMC8.5 at various temperatures. P_{O_2} dependencies of the electronic conductivities in LSGMC8.5 also depend strongly on working temperatures. At temperatures higher than 1073 K, the P_{O_2} dependencies of free electron conductivity and electron hole conductivity are about −1/4 and 0.07, respectively. However, the P_{O_2} dependency of free electron conductivity is only about −0.13 at 973 K. Further, the P_{O_2} dependency of electron hole conductivity at 973 K is significantly different from that at higher temperatures, and it even shows no P_{O_2} dependency at relatively high oxygen partial pressures.

Temperature dependencies of the electronic conductivities of various samples are shown in Fig. 9. Because the characteristics of electronic conductivities at 973 K are different from those

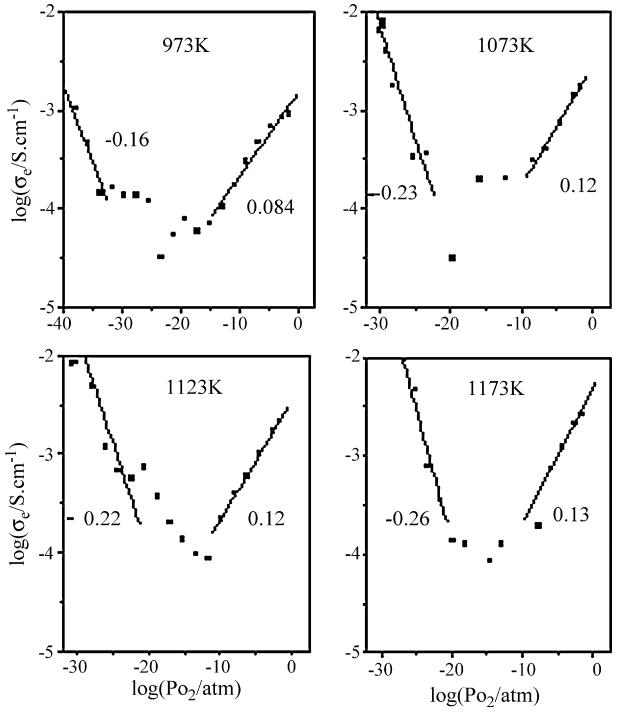

Fig. 7. Electronic conductivities in LSGMC5 as a function of oxygen partial pressure at various temperatures.

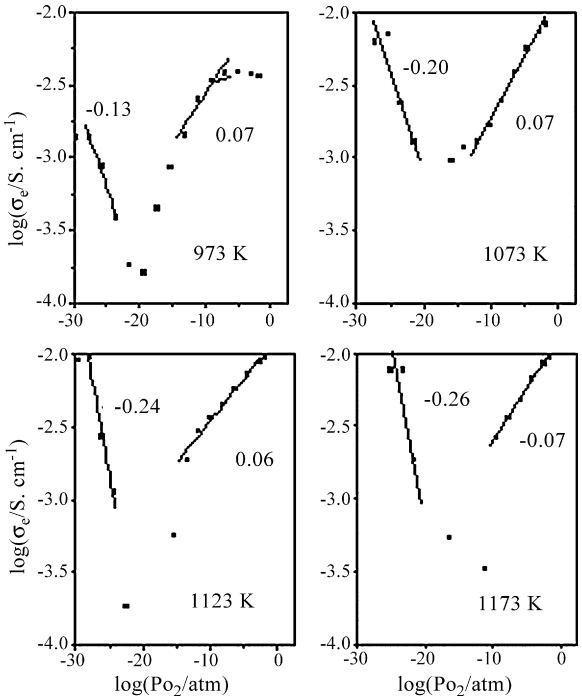

Fig. 8. Electronic conductivities in LSGMC8.5 as a function of oxygen partial pressure at various temperatures.

at higher temperatures for LSGMC5 and LSGMC8.5, the temperature range analyzed in Fig. 9 is 1073–1173 K. Moreover, because the electronic conductivities in various samples have strong dependency on oxygen partial pressure, electronic conductivities at two typical oxygen partial pressures, i.e., 1 atm and 10^{-25} atm are analyzed, which correspond to electron hole conduction and free electron conduction, respectively. Activation energies of the electronic conductivities of various samples can

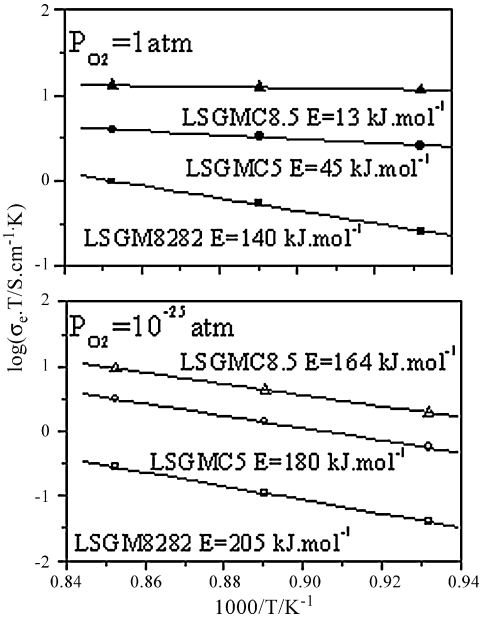

Fig. 9. Temperature dependencies of the electronic conductivities in LSGM-8282, LSGMC5 and LSGMC8.5 at 1 atm and 10^{-25} atm oxygen partial pressures, respectively.

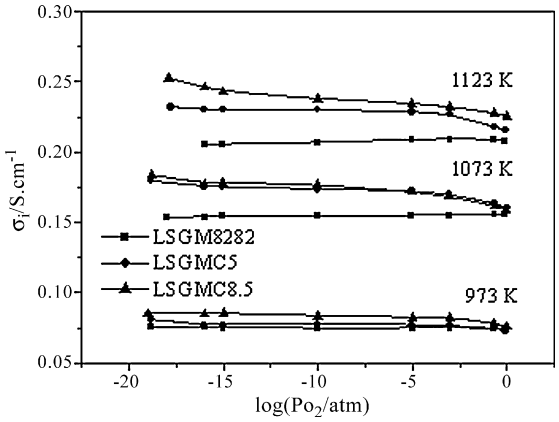

Fig. 10. Oxygen ion conductivities in LSGM8282, LSGMC5 and LSGMC8.5 as a function of oxygen partial pressure at various temperatures.

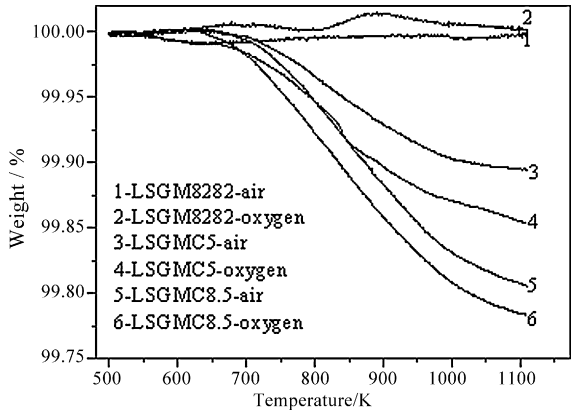

Fig. 11. Weight losses of LSGM8282, LSGMC5 and LSGMC8.5 as a function of temperature in flowing high purity nitrogen.

be calculated from the slope of the curves in Fig. 9. It is clear that both the activation energies of electron hole conductivity and free electron conductivity decrease with increasing concentration of cobalt. Further, the activation energies of the electron hole conductivity are much lower than those of free electron conductivity, agreeing with the results in the literatures [7,8,16].

3.4. Oxygen ion conductivity

Oxygen ion conductivity can be calculated from the difference between the electrical conductivity and electronic conductivity. Oxygen ion conductivities in LSGM8282, LSGMC5 and LSGMC8.5 at 973, 1073, and 1123 K at various oxygen partial pressures are shown in Fig. 10. Oxygen ion conductivities of various samples are in the order of LSGM8282 < LSGMC5 < LSGMC8.5. It is clear that cobalt is effective in improving the oxygen ion conductivity of LSGM8282. It can be further seen from Fig. 10 that the oxygen ion conductivity in LSGM8282 has no dependency on oxygen partial pressure. However, the oxygen ion conductivities of LSGMC5 and LSGMC8.5 increase obviously with the decrease in oxygen partial pressure especially in high and low oxygen partial pressure region. It is clear that the dependency of electrical conductivity on oxygen partial pressure shown in Section 3.2 is caused by the dependency of oxygen ion conductivity on oxygen partial pressure.

3.5. Thermo-gravimetric analyses

The weight losses of LSGM8282, LSGMC5 and LSGMC8.5 as a function of temperature were measured using thermo-gravimetric analyses to determine the change in oxygen vacancy concentration of the samples, which could illuminate the reason leading to the dependency of oxygen ion conductivity on oxygen partial pressure.

Shown in Fig. 11 is the relative weight of various samples as a function of temperature in flowing high purity nitrogen. The weight of LSGM8282 does not change with temperature, demonstrating that the composition of LSGM8282 is rather stable and there is no change in the concentration of oxygen vacancy. On the other side, obvious weight losses of LSGMC5 and LSGMC8.5 are observed with the increase in temperature. Moreover, the weight losses of LSGMC5 and LSGMC8.5 pre-treated in oxygen are higher than those pre-treated in air, and the weight loss of LSGMC8.5 is higher than that of LSGMC5. These results demonstrate that the concentration of oxygen vacancy in LSGMC5 and LSGMC8.5 increases with the decrease in oxygen partial pressure [8].

Table 1
The change in sample weight ($\Delta m\%$), valance of Co (ΔV_{Co}), and oxygen stoichiometry ($\Delta\delta$ in $3-\delta$) of different samples in nitrogen assuming that the initial valence of Co is +3

Electrolyte	$\Delta m\%$	ΔV_{Co}	$\Delta\delta$
LSGM8282-air	0	0	0
LSGM8282-oxygen	0	0	0
LSGMC5-air	−0.10	−0.60	0.015
LSGMC5-oxygen	−0.13	−0.76	0.019
LSGMC8.5-air	−0.19	−0.66	0.028
LSGMC8.5-oxygen	−0.21	−0.73	0.031

The change in the valance of cobalt and the oxygen stoichiometry are calculated and shown in Table 1 assuming that the initial valences of La, Sr, Ga, Mg, Co and O are +3, +2, +3, +2, +3 and −2, respectively [8]. Cobalt in the electrolyte could exhibit variable valence, therefore the calculation is also carried out assuming that the initial valence of cobalt is +4. The results show that the variation of the initial valence of cobalt has no obvious effect on the results, and the maximum relative error is less than 1%.

Table 1 shows that the change in the valence of cobalt and oxygen stoichiometry in LSGMC5 and LSGMC8.5 pre-treated in air are lower than those pre-treated in oxygen. For the samples treated in the same atmosphere, the change in the valence of cobalt is similar for LSGMC5 and LSGMC8.5, while the change in oxygen stoichiometry of LSGMC5 is lower than that of LSGMC8.5.

4. Discussion

The results in this study demonstrate that both the temperature dependency and oxygen partial pressure dependency of the

electronic conductivity of cobalt doped lanthanum gallate are different from those of LSGM8282. The addition of cobalt into LSGM8282 also leads to a change in the oxygen partial pressure dependency of oxygen ion conductivity.

Oxygen partial pressure dependencies of free electron and electron hole conductivity in LSGM8282 are −1/4 and 1/4, respectively, suggesting that the generation of free electron and electron hole charge carriers can be described as Eqs. (9) and (10), respectively [10].

$$\tfrac{1}{2}O_2 + V_O^{\bullet\bullet} = O_O^X + 2h^\bullet \quad \text{for electron hole conduction} \tag{9}$$

$$O_O^X = V_O^{\bullet\bullet} + \tfrac{1}{2}O_2 + 2e' \quad \text{for free electron conduction} \tag{10}$$

Oxygen partial pressure dependencies of the free electron and electron hole conductivity of LSGMC5 are about −1/4 and 1/8, respectively, within the temperature range of 1073–1173 K. P_{O_2} dependency of the electron hole conductivity of LSGMC8.5 is even lower than that of LSGMC5. These results illustrate that the mechanism of the generation of electron hole in cobalt doped LSGM8282 could be different from that of Eq. (9). Ishihara et al. [8] proposed Eq. (11) to explain the P_{O_2} dependency of the electron hole conduction in LSGMC5 based on the fact that the average valence number of Co in LSGMC5 decreased from about +3 to +2 with decreasing oxygen partial pressures in high oxygen partial pressure region. However, they did not analyze the characteristics of the electron hole generation process described by Eq. (11).

$$Co'_{Ga} + V_O^{\bullet\bullet} + \tfrac{1}{2}O_2 = Co_{Ga}^X + O_O^X + h^\bullet \tag{11}$$

Eq. (11) cannot be analyzed straightforward, because the concentrations of $V_O^{\bullet\bullet}$, Co'_{Ga}, Co_{Ga}^X and $h^\bullet$ change with oxygen partial pressure. Further, the initial values of all the defects in Eq. (11) are also not available. Here, the electron hole generation process controlled by Eq. (11) is discussed under some limiting conditions.

Assuming that (1) the average valance number of cobalt in LSGMC5 is +2 at low oxygen partial pressures within the temperature range of 1073–1173 K, (2) there is no strong interaction among the defects in LSGMC5, and (3) the amount of electron hole generated by Eq. (11) is much larger than that by Eq. (9) at high oxygen partial pressures. Then, the concentrations of Co'_{Ga}, $V_O^{\bullet\bullet}$, Co_{Ga}^X and $h^\bullet$ in LSGMC5 could be estimated as 0.05, 0.2, 0, and 0 M, respectively, at low oxygen partial pressures. The first assumption is justified by the results reported by Ishihara et al. [8]. The second assumption is acceptable considering the high temperature investigated. The third assumption is also reasonable if assuming that the large difference in electron hole conductivity between LSGM8282 and LSGMC5 is mainly due to the difference in the number of charge carriers, i.e., electron holes. Further, a significant change in the valence number of Co is observed with decreasing oxygen partial pressures as shown in Table 1, suggesting that the extrinsic electron holes generated could be the dominant electron hole charge carriers at an oxygen partial pressure higher than 1×10^{-5} atm.

With the increase in oxygen partial pressure, the concentrations of Co'_{Ga} and $V_O^{\bullet\bullet}$ decrease, and the concentrations of Co_{Ga}^X and $h^\bullet$ increase. Assuming that the change in the concentration of Co'_{Ga} is x at some fixed oxygen partial pressure, the equilibrium of Eq. (11) can be described using Eq. (12).

$$\frac{x^2}{(0.05-x)(0.2-x)P_{O_2}^{1/2}} = K \tag{12}$$

Here, K is the equilibrium constant of Eq. (11). The solution of Eq. (12) is

$$x = \frac{-0.25KP_{O_2}^{1/2} \pm \sqrt{0.0225K^2P_{O_2} + 0.04KP_{O_2}^{1/2}}}{2(1-KP_{O_2}^{1/2})} \tag{13}$$

Oxygen partial pressure dependency of x cannot be obtained straightforward from Eq. (13). However, Eq. (13) can be simplified as Eqs. (14) and (15) under limiting conditions.

$$x = 0.2 \text{ or } 0.05, \quad KP_{O_2}^{1/2} \gg 1 \tag{14}$$

$$x = \frac{1}{10}K^{1/2}P_{O_2}^{1/4}, \quad KP_{O_2}^{1/2} \ll 1 \tag{15}$$

Because the concentration of Co_{Ga}^X should be less than or equal to 0.05 according to the stoichiometry of LSGMC5, x should be 0.05 under the condition that $KP_{O_2}^{1/2} \gg 1$. Eq. (14) demonstrates that the concentration of electron hole should be independent of oxygen partial pressure under the condition that $KP_{O_2}^{1/2} \gg 1$, i.e., at high oxygen partial pressures. On the other hand, the concentration of electron hole is proportional to $P_{O_2}^{1/4}$ under the condition that $KP_{O_2}^{1/2} \ll 1$, i.e., at relatively low oxygen partial pressures. Assuming that the mobility of electron hole has no obvious dependency on its concentration, the oxygen partial pressure dependency of the electron hole conductivity should be within the range of 0–1/4. Therefore, it is reasonable to observe a about 1/8 P_{O_2} dependency of the electron hole conductivity in this study.

A P_{O_2} related P_{O_2} dependency of electron hole conductivity is expected if Eq. (11) is the dominant process for the generation of electron holes. The P_{O_2} dependency of electron hole conductivity would be 0 at high oxygen partial pressures, and increase to 1/4 at low oxygen partial pressures. The results in Figs. 7 and 8 show clearly that the P_{O_2} dependencies of electron hole conductivity in LSGMC5 and LSGMC8.5 decrease with increasing oxygen partial pressures at 973 K. The activation energies of the electron hole conductivity of LSGMC5 and LSGMC8.5 are much lower than that of LSGM8282, suggesting that the electron holes generated by Eq. (11) could play an important role at low temperatures [8]. Therefore it is reasonable to observe the P_{O_2} dependent P_{O_2} dependency of electron hole conductivity at low temperatures. Eq. (11) also suggests that the concentration of oxygen vacancy should increase with decreasing oxygen partial pressures especially in high oxygen partial pressure region [7,8], which is verified by the thermo-gravimetric analyses.

The concentrations of oxygen vacancy in LSGMC5 and LSGMC8.5 in oxygen are estimated from the stoichiometry of the materials by assuming that the valence of Co is +2, +3 and +4, respectively. The concentrations of oxygen vacancy in LSGMC5 and LSGMC8.5 in air or high purity nitrogen are estimated using

Table 2
Oxygen ion conductivity (σ_i (S cm^{-1})) and the estimated molar concentration of oxygen vacancy in LSGMC5 and LSGMC8.5 pretreated under various atmospheres at 1073 K[a]

Electrolyte	$[V_O^{\bullet\bullet}](Co^{2+})$	$[V_O^{\bullet\bullet}](Co^{3+})$	$[V_O^{\bullet\bullet}](Co^{4+})$	σ_i (S cm^{-1})
LSGMC5-oxygen	0.200	0.175	0.150	0.160
LSGMC5-air	0.204	0.179	0.154	0.163
LSGMC5-nitrogen	0.219	0.194	0.169	0.172
LSGMC8.5-oxygen	0.200	0.157	0.115	0.159
LSGMC8.5-air	0.203	0.160	0.118	0.162
LSGMC8.5-nitrogen	0.221	0.178	0.136	0.172

[a] $[V_O^{\bullet\bullet}](Co^{2+})$, $[V_O^{\bullet\bullet}](Co^{3+})$ and $[V_O^{\bullet\bullet}](Co^{4+})$ are the estimated molar concentrations of oxygen vacancy assuming that the initial valence of Co in oxygen is +2, +3 and +4, respectively.

the results of thermo-gravimetric analyses [17] shown in Table 1. As shown in Table 2, both the concentration of oxygen vacancy and oxygen ion conductivity increase with the decrease in oxygen partial pressure, suggesting a strong dependency of oxygen ion conductivity on the concentration of oxygen vacancy.

The increase in the concentration of oxygen vacancy should lead to an increase in oxygen ion conductivity assuming that the mobility of oxygen vacancy does not change dramatically under the experimental conditions. However, the ratio of the oxygen ion conductivity in oxygen or air to that in nitrogen is lower than the corresponding value of the concentration of oxygen vacancy for both LSGMC5 and LSGMC8.5. For an example, the ratio of the oxygen ion conductivity of LSGMC5 in high purity nitrogen to that in oxygen and air is 1.075 and 1.055, respectively. However, the ratio of the concentration of oxygen vacancy of LSGMC5 in high purity nitrogen to that in oxygen and air is 1.095 and 1.074, respectively, even assuming that the initial valence of Co in oxygen is +2. The discrepancy between the increase in oxygen ion conductivity and the increase in the concentration of oxygen vacancy illustrates that part of the oxygen vacancies could aggregate with each other or with other species, which decreases the mobility. However, it is clear that the increase in the number of oxygen vacancy could be responsible for the increase in oxygen ion conductivity with decreasing oxygen partial pressures.

5. Conclusions

Electrical conductivities in $La_{0.8}Sr_{0.2}Ga_{0.8}Mg_{0.15}Co_{0.05}O_{3-\delta}$ (LSGMC5) and $La_{0.8}Sr_{0.2}Ga_{0.8}Mg_{0.115}Co_{0.085}O_{3-\delta}$ (LSGMC8.5) increased with decrease in oxygen partial pressure especially in the high ($>10^{-5}$ atm) and low oxygen partial pressure regions ($<10^{-15}$ atm). However, the conductivity in $La_{0.8}Sr_{0.2}Ga_{0.8}Mg_{0.2}O_{3-\delta}$(LSGM8282) showed no dependency on oxygen partial pressure. At temperatures higher than 1073 K, P_{O_2} dependencies of the free electron conductivities in LSGM8282, LSGMC5 and LSGMC8.5 were about −1/4, and the P_{O_2} dependencies of the electron hole conductivities were about 0.25, 0.12, and 0.07, respectively. The decrease in the valance of cobalt and the increase in the concentration of oxygen vacancy with decreasing oxygen partial pressures were the main reason leading to the abnormal oxygen partial pressure dependency of oxygen ion conductivity and electron hole conductivity. Both the electronic conductivity and oxygen ion conductivity in cobalt doped lanthanum gallate samples increased with increasing concentration of cobalt, suggesting that the concentration of cobalt should be optimized carefully to maintain a high electrical conductivity and close to a oxygen ion transference number of 1.

Acknowledgements

This material is based upon work supported by the “Fujian Province Science and Technology Program, Key Project (No. 2003H046)” and Research Fund for Homecoming scholars.

References

[1] N.Q. Minh, J. Am. Ceram. Soc. 76 (1993) 563–588.
[2] T. Takahashi, K. Ito, H. Iwahara, Electrochim. Acta 12 (1967) 21–30.
[3] J.W. Fergus, J. Power Sources 162 (2006) 30–40.
[4] J.B. Goodenough, Solid State Ionics 94 (1997) 17–25.
[5] A. Skowron, P.N. Huang, A. Petric, J. Solid State Chem. 143 (1999) 202–209.
[6] N. Trofimenko, H. Ullmann, Solid State Ionics 124 (1999) 263–270.
[7] T. Ishihara, S. Ishikawa, C. Yu, T. Akbay, K. Hosoi, H. Nishiguchi, Y. Takita, Phys. Chem. Chem. Phys. 5 (2003) 2257–2263.
[8] T. Ishihara, S. Ishikawa, M. Ando, H. Nishiguchi, Y. Takita, Solid State Ionics 173 (2004) 9–15.
[9] T. Kawada, T. Horita, N. Sakai, B.A. van Hassel, H. Yokokawa, M. Dokiya, ISSI Lett. 4 (2) (1993) 6–7.
[10] J.H. Kim, H.I. Yoo, Solid State Ionics 140 (2001) 105–113.
[11] S. Wang, X. Lu, M. Liu, J. Solid State Electrochem. 6 (2002) 384–388.
[12] S. Wang, Acta Physico-Chimica Sinica 20 (1) (2004) 43–46.
[13] J.B. Wagner, C. Wanger, J. Chem. Phys. 26 (1957) 1597–1601.
[14] M.H. Hebb, J. Chem. Phys. 20 (1952) 185–190.
[15] I. Riess, Solid State Ionics 91 (1996) 221–232.
[16] J.H. Jang, G.M. Choi, Solid State Ionics 154/155 (2002) 481–486.
[17] K. Kawamura, K. Watanabe, Y. Nigara, A. Kaimai, T. Kawada, J. Mizusaki, J. Electrochem. Soc. 145 (1998) 2552–2558.